Lignin catalytic hydroconversion in a semi-continuous reactor: An experimental study

Junjie Pu[a,b], Thanh-Son Nguyen[a], Emmanuel Leclerc[a], Chantal Lorentz[a], Dorothée Laurenti[a,*],
Isabelle Pitault[b], Mélaz Tayakout-Fayolle[b], Christophe Geantet[a]

[a] Univ. Lyon, IRCELYON, CNRS-UCB Lyon 1, UMR5256, 2 avenue A. Einstein, 69626, Villeurbanne cedex, France
[b] Univ Lyon, Université Claude Bernard Lyon 1, CNRS, LAGEP UMR 5007, 43 boulevard du 11 novembre 1918, F-69100, Villeurbanne, France

ARTICLE INFO

ABSTRACT

The valorization of lignin coming from pulp industry or bio-ethanol refineries into renewable chemicals is one of the great challenges of the biorefinery concept. Among the several processes proposed to depolymerize lignin, catalytic hydroconversion appeared efficient to get high liquid yield and can provide targeted aromatic monomers. A new semi-continuous set-up consisting in a batch reactor opened on the gas-phase was implemented to carry out the catalytic lignin liquefaction into phenolic and deoxygenated aromatic compounds with continuous H$_2$ feeding. The interest of this equipment is the continuous removing of light products and water from the reacting mixture whereas the hydrogen donor solvent is reintroduced in the reactor via a reflux/condensing system. A Co-promoted Mo sulfide catalyst was used and thanks to efficient separation and extensive analysis, the components of the different gaseous, liquid and solid fractions obtained were identified and quantified. The evolution of the various fractions in function of the time and the deep investigation of the composition, allowed to propose a reaction scheme for the lignin depolymerization in those operating conditions.

1. Introduction

The increase of energy demand and the international concerns about protection and preservation of the environment, combined with the need of becoming independent from fossil resources suppliers, urge the scientists to find new renewable solutions to provide alternative chemicals and fuels in a near future. Among the possible alternatives to fossil oils, lignocellulosic biomass is a highly available neutral carbon resource that can bring a broad range of chemicals and materials. It is now well admitted that the valorization of lignin co-produced during cellulose extraction for pulp industry or with cellulosic ethanol in biorefinery is a key-step to increase sustainability and competitiveness of those industries [1]. Effectively, over the 50–60 million tons of lignin co-produced each year with cellulose, it has been proposed that a great part could be treated in a second efficient valorization process while the other part would be still burned as a low value-fuel to afford heat power to the industry [2]. Lignin, which represents almost 20–30 % of lignocellulosic biomass is the most relevant and abundant renewable resource to produce aromatics due to its original polymeric structure composed by methoxy- and hydroxy-phenylpropane units with ether linkages [3,4]. The use of lignin as a precursor of aromatic hydrocarbons or phenolic compounds has gained a strong interest due to its relative low cost and increasing availability. However, the transformation of lignin is a delicate topic due to the complexity of the lignin structure which is varying according to its origin and is already modified during the fragmentation process [5]. Thus, the liquefaction of lignin is first facing analytical problems of the initial lignin material and then those of the complex mixtures of products obtained after conversion. In order to find a catalytic way to valorize co-produced lignin, many type of thermochemical processes have been already proposed for lignin liquefaction [6,7] using either oxidative [8] or reductive [9] atmosphere and also investigating the effect of various solvents including H-donor solvents [10,11]. Inspired by early works [12–14], we previously proposed the catalytic hydroconversion as a mean to liquefy lignin and produce aromatics [15,16]. The reaction took place in a H-donor solvent which allows to prevent condensation reactions due to radical reactions between the fragments and also improves hydrogen diffusion into the liquid phase where the catalysis stages happened. Even in the presence of H-donor solvent, hydrogen partial pressure can rapidly decrease in a batch reactor detrimentally to the hydrogenolysis process. Semi-continuous reactors under H$_2$ flow were thus proposed in literature to circumvent this problem [13,17]. In

this study, the depolymerization of a wheat straw soda lignin was undertaken via catalytic hydroconversion with the main target to investigate the selectivity towards aromatics (BTX) or phenolics which are representing an important market value, according to recent report [18].The best yields of phenolics and aromatics obtained until now from technical lignins in reductive conditions are in the range 20 wt% - 35 wt% in solvent-free catalytic systems from kraft lignin [19] or pyrolytic forestry residue lignin [20]. Until 23 wt% of monomers were obtained from a wheat straw Protobind lignin, using a CuMgAlOx catalyst in supercritical ethanol [21]. However, in this case, the solvent reacts with the products. Of course, these yields greatly depend on the type of lignin utilized. We must admit that the wheat straw soda lignin used in this work is not the best candidate for producing aromatic monomers [22] but the second target is to provide experimental values to establish a kinetic model. In order to reach these goals and to evaluate clearly the catalyst impact, we propose the utilization of a semi-continuous batch reactor, opened on the gas phase with a continuous feeding of H_2, equipped with a reflux system for recycling the H-donor solvent in the reactor and removing continuously light products and water from the reacting mixture. Thanks to this reactor, we obtained a rapid separation of deoxygenated monomers which are recovered in the condenser/separator system and limit an over-conversion of this products. We used here a well-known industrial extruded alumina supported CoMoS catalyst in order to facilitate the separation with the solid-derivatives and to recover it after reaction for analysis. All the fractions were characterized by various techniques, and when it was possible, the composition was comprehensively investigated to follow the evolution of families of compounds with the conversion. Based on these experimental results, an overall reaction scheme is proposed and has been further used to build up a kinetic model [23].

2. Experimental: materials and methods

2.1. Materials

Protobind 1000 lignin was produced by soda pulping of wheat straw and was supplied by Green Value (Switzerland) as a brown dry powder. Lignin was dried at 80 °C in vacuum oven before use. The reagents used for the reaction, products-recovery and analytical purposes were 1,2,3,4-tetrahydronaphthalene (tetralin) (Sigma-Aldrich, ReagentPlus®, 99%), acetone (Sigma-Aldrich, Chromasolv®, for HPLC, ≥ 99.9%), pyridine (Carlo Erba, purum, ≥ 99.9%), acetic anhydride (Prolabo, analytical grade), tetrahydrofuran (Sigma-Aldrich, analytical grade, ≥ 99.9%), n-heptane (Carlo-Erba, 99.2% pure) and 2-chloro-4,4,5,5-tetramethyl-1,3,2-dioxaphospholane (Sigma-Aldrich, 95%), CDCl$_3$ (Sigma-Aldrich, 99.8% atom D), DMSO-d6 (Sigma-Aldrich, 99.9% atom D). The compounds used as reference compounds for products identification by gas chromatography (hydrogen, carbon monoxide, carbon dioxide, methane, ethane, propane, n-butane, isobutane, pentane, isopentane, hexane, 2-methylpentane, ethylene, propylene, 1-butene, 1,3-butadiene, 1-pentene, 1-hexene), were of analytical grade.

The catalyst used in this study was an industrial CoMo catalyst supported over γ-alumina (shaped as extrudates length: 2–10 mm, diameter: 1.2 mm) composed by CoO (3 wt%), MoO$_3$ (14 wt%), with a total pore volume of 0.5 cm^3/g, an average pore diameter of 7.9 nm and the BET surface area was 193 m^2/g. Activation of the catalyst was performed ex situ at 400 °C (ramp of 5 °C/min) for 150 min under a flow (4 L/h) of H_2/H_2S (15 vol% H_2S).

2.2. Characterizations

For C, H, O, N and S content measurements, a Thermo Scientific Flash 2000 apparatus was used. Oxygen was measured after pyrolysis by quantification of CO using a thermal conductivity detector. Carbon, hydrogen, nitrogen and sulfur were measured after combustion and separation of CO$_2$, H$_2$O, NOx and SO$_2$ respectively, and quantification

of these gases by a thermal conductivity detector. Other elemental analyses (metals) were performed by ICP-AES, using an Activa apparatus from Horiba Jobin Yvon, after solubilization of samples in acidic solutions.

Gel permeation chromatography (GPC) analyses were based on previously developed methods for lignin molecular weight determination [24]. Analyses were performed by using an Agilent apparatus (1200 series) equipped with two PL gel columns (50 and 500 Å) and a differential refractive index (DRI) detector. Analyses were carried out at 35 °C using THF as eluent at a flow rate of 1 mL/min. Each sample was dissolved at circa 1 wt% in THF and filtered (0.4μm) before injection. The GPC system was calibrated with polystyrene (PS) standards with molecular weights from 162 to 55,100 g.mol^{-1}. Depicted chromatograms were normalized to detector response. Lignin was analyzed by direct solubilization in THF and also after acetylation step, in order to improve its solubility in THF and check GPC distribution. The lignin residues obtained after each hydroconversion run were completely soluble in THF and acetylation was not carried out in this case.

^{31}P *NMR* technique was used for the characterization and the quantification of OH groups on the basis of previously developed methods involving a prior derivative phosphitylation step [25,26]. Samples were accurately weighted (c.a. 30 mg) and dissolved in a solution containing 200 mg of pyridine, 100 mg of an internal standard solution in pyridine (cyclohexanol, 15.7 mg/g), 100 mg of 2-chloro-4,4,5,5-tetramethyl-1,3,2-dioxaphospholane, and 200 mg of CDCl$_3$. ^{31}P-NMR data were obtained with Bruker Avance HD 400 (400.13 MHz (^{1}H), 100.61 MHz (^{13}C) equipped with a BBFO 5 mm probe. The phosphorous atoms bounded to former alcohol or phenols have different chemical shifts that enable to quantify each OH group [25].

The ^1H, ^{13}C *NMR* techniques enable basic structural quantitative characterizations. These NMR experiments were carried out on a Bruker Avance III spectrometer operating at 1000.30 MHz (proton resonance frequency) equipped with a 5 mm TCI cryo-probe. Around 50 mg of sample was dissolved in 700 mg of DMSO-d$_6$. ^{1}H spectra were acquired with single pulse acquisitions at 1000.30 MHz, ^{13}C spectra with inverse gated decoupling at 25.52 MHz at 323 K.

The μGC-TCD technique was used to characterize gases formed during lignin hydroconversion. Analyses were performed every 3 min during each run. We used a R-series SRA system equipped with three analytical modules. A 5 Å molecular sieve column (10 m, 12 μm) was used to analyze H$_2$, CH$_4$ and CO; the carrier gas was argon; the backflush injector temperature was maintained at 80 °C and the column temperature was also kept at 80 °C. A Poraplot U column (8 m, 30 μm) was used to separate CO$_2$, ethane, ethylene and H$_2$S; the carrier gas was hydrogen; the backflush injector temperature was maintained at 90 °C and column temperature was kept constant at 80 °C. A OV-1 column (8 m, 2 μm) was used to analyze C3 to C6 hydrocarbons; the gas carrier was hydrogen; injection temperature was maintained at 90 °C, while column temperature was kept constant at 70 °C. The three modules were equipped with TCD detectors and quantification was performed from the calibration of each gas using reference mixtures. H$_2$ consumption was obtained by the difference between H$_2$ introduced and remaining.

Two-dimensional gas (GC × GC) MS chromatograms were recorded using an Agilent 6890 apparatus with a liquid nitrogen cryogenic jet modulation from Zoex Corporation equipped with two parallel detectors, a FID and a quadrupole MS detector (Agilent 5975B, Scan parameters: from 45 to 300 m/z at 22 scan/s) [27]. The combination of columns was adapted from the reverse system proposed for the analysis of phenols and oxygenates in coal derived liquid [28]. The first column was a moderately polar VF1701 column (30 m × 0.25 mm × 0.25 μm) and the second column was an apolar DB1 column (2 m × 0.1 mm × 0.1 μm). The temperature program of the first oven started at 50 °C for 5 min and then was heated up at 1.75 °C/min until 300 °C. The second oven started at 50 °C for 0 min and then heated up at 1.8 °C/min until 307 °C and at 1.8 °C/min until 320 °C. The modulation time was 12 s

and the modulator hot jet temperature was set to 280 °C. The raw signal is a time-ordered series of second dimension chromatograms and it is transferred to GC Image™ software with the value of the modulation period, which constructs a two-dimensional chromatogram by placing the two chromatograms side by side. Identification is realized by cross referencing the measured mass spectra to the spectra in the available MS libraries. Quantification was done with FID analysis taking into account an effective carbon number for each family of compounds relatively to aniline as internal standard (ECN quantification method) [29].

Karl-Fischer titration method was used to determine the water content in a sample. Analyses were performed with a Metrohm Titrando 852 via coulometric titration. Before each analysis, the sample (organic phase or aqueous phase) was diluted with THF in order to make its concentration of water around 300 ppm.

2.3. Characterization of the used catalyst

After each catalytic reaction, the catalysts were recovered and characterized by N_2-adsorption isotherms (using standard methods), CHONS and XPS.

The X-ray photoelectron spectroscopy (XPS) experiments were carried out in a KRATOS AXIS Ultra DLD spectrometer equipped with a hemispherical analyzer operating at a fixed pass energy of 40 eV and working under vacuum ($< 10^{-9}$mbar). Before analyses, the samples were freshly sulfided and transferred into the spectrophotometer under argon atmosphere. All the data were acquired using monochromatic Al Kα radiation (1486.6 eV,150 W), and the binding energies (BE) were corrected taking C 1s (284.6 eV) as reference. The surface area analyzed on the sample was 300 μm × 700 μm and allows a representative characterization of the whole sample. The Mo 3d, Co 2p, S 2p, Al 2p, O 1s spectra were treated using the software "XPS processing" and applying a Shirley background subtraction and Gaussian–Lorentzian decomposition parameters with 30/70 Gaussian/Lorentzian proportion.

2.4. Catalytic unit and procedure

Catalytic hydroconversion experiments were carried out in an upgraded semi-continuous pilot (Fig. 1) which consists in a batch Parr reactor (300 ml) opened on the gas phase. H_2 is continuously fed in the reactor thanks to a mass flowmeter (40 N L/h) and a reflux system allows to remove continuously lights products and water from the reacting mixture. While the reactor temperature is 350 °C, the temperature of this reflux system was set at 160 °C to remove only deoxygenated aromatics and some small phenols and recycle the tetralin used as a H-donor solvent. After the reflux system, a couple of condensers and separators (cold traps at 15 °C and 4 °C) allowed to recover light liquid products. A Coriolis Flow Meter and a pressure controller permit respectively to quantify the gases online and control the total pressure. The gases were analyzed online thanks to a μ-GC analyzer.

For each run, wheat straw soda lignin (Protobind 1000) from Green Value was introduced (30 g) with tetralin (70 g) and freshly sulfided CoMoS/Al_2O_3 (3 g) in the unit. After removing air from the reactor by flushing H_2 three times at 1 MPa, the temperature was increased up to 350 °C and H_2 was introduced to reach to the total pressure of 8 MPa. Approximately 35–38 min were needed to reach those operating conditions. The reaction time was measured from this time defined as t0 point (t = 0 at 8 MPa and 350 °C). During the run, the set-up temperature and pressure were controlled and kept constant, and the stirring rate was set at 800 rpm. After the chosen reaction time, the temperature was decreased and a fast depressurization of the pilot was started when the reactor was cooled down to 160 °C using an ice bath. The liquid in the condenser/separator part and in the reactor were recovered and weighted. The overall mass balance was carefully determined and was higher than 96 wt% ± 2 wt% for each experiment, including the consumed hydrogen.

A product recovery protocol developed previously was applied to separate the liquid/solid fractions [15, Graphical guide in suppl. mat.]. Liquid (from the batch reactor) and solid were separated by centrifugation and solids were extracted with THF using a Soxhlet apparatus. The so-called "lignin residue" is the THF soluble fraction corresponding to partially converted lignin. The remaining liquid is composed of monomers and oligomers which are similar to lignin residue but soluble in tetralin mixture. Thanks to a precipitation step with heptane [16], this fraction was separated by filtration and analyzed. The liquid from the separator/condenser system was composed of an aqueous phase and an organic phase which separated spontaneously. The two distinct phases were analyzed and quantified. For each residence time, the lignin residues were analyzed by GPC and ^{13}C, ^{1}H, ^{31}P NMR, the monomers in the liquid were characterized by GCxGC-MS for identification and GCxGC-FID for quantification. The whole liquid containing also oligomers was also analyzed by GPC.
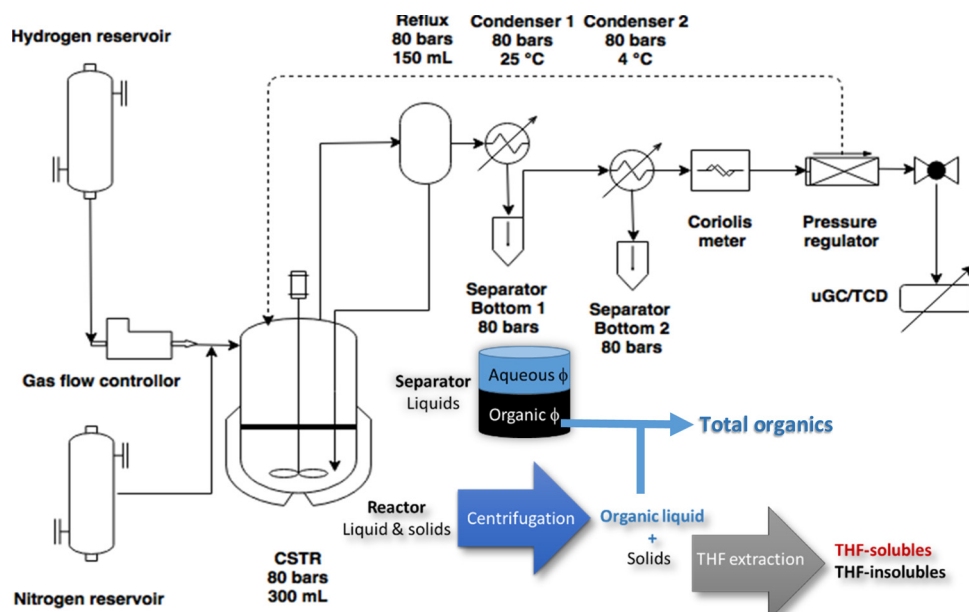

Fig. 1. Catalytic reactor system used in this study and shortened products-recovery protocol.

Table 1

Elemental analyses, ashes, water (from TGA) and O/C, H/C atomic ratios for the initial lignin P1000.

wt%	Lignin P1000	THF-soluble fraction (91 wt%)	THF-insoluble fraction (9 wt%)
C	61.1	63.2	39.0
H	5.7	6.2	3.6
O	29.9	28.5	35.9
N	0.7	0.7	0.9
S	0.9	0.8	5.1
Ashes	3.1	n.d.	n.d.
Water	2.1	n.d.	n.d.
Total	103.4	99.4	84.6
Atomic ratios			
H/C	1.12	1.18	1.11
O/C	0.37	0.34	0.69

For all the runs, the yields were calculated in wt% based on ash-free and moisture-free lignin:

$$Yield\ (wt\%) = \left(\frac{w(i)}{w(lignin - ashes - moisture)} \right) x\ 100$$

Where w (i) is the weight of the product i

And w (lignin – ashes -moisture) the weight of initial lignin deduced of ashes and water content obtained by TGA analysis.

3. Results and discussion

3.1. Lignin characterization

First of all, characterization of initial P1000 lignin was undertaken by CHONS, TGA (Fig. 8, suppl. mat.), ^{13}C, ^{1}H and ^{31}P NMR (data given in Table 1, Tables S1, S2, S3 in suppl. mater. respectively). We can first note that unlike ^{1}H NMR where superposition of peaks avoid the quantification of the 3–6 ppm region, all the carbon was quantified by ^{13}C NMR, as the total detected carbon is 51.2 mmol/g of lignin corresponding to 62.5 wt%, which is in accordance with the C elemental analysis result (61.1 wt%) of the starting material. By crossing those different analytical results, we can confirm and deduce several complementary data which are precious for the understanding of the conversion and have been summarized in Table S4 (suppl. mater.). For instance, initially total phenolic OH (hydroxyphenolic, guaiacyl and syringyl) represent 3.8 mmol per g of lignin (^{31}P NMR); this value is in accordance with the 3.7 mmol/g found by ^{1}H NMR. Methoxy groups are quantified at 4.8 mmol/g by ^{13}C NMR (this value can be compared with 5.3 mmol/g found with ^{31}P NMR if we sum guaiacyl (1 methoxy) and syringyl (2 methoxy, but the condensed phenolic units also detected in this region induced an error for this value)). Using ^{13}C NMR, 11.5 mmol/g of $C_{aromatic}$—O were detected, including C_{arom}—OH and C_{arom}—O—R, R being aromatic or aliphatic moiety. We know that the respective quantity of C_{arom}—OH and C_{arom}—OCH$_3$ are 3.8 mmol/g and 4.8 mmol/g. $C_{aliphatic}$—O (including C_{aliph}—OH and C_{aliph}—O—C without methoxy groups) are quantified at 2.5 mmol/g and $C_{aliphatic}$—OH, 1.5 mmol/g by ^{31}P NMR, thus we can deduce that $C_{aliphatic}$—O—C_{arom} are around 1 mmol/g in the initial material. Then the 11.5 mmol/g of C_{arom}—O can be divided into: C_{arom}—OH: 3.8 mmol/g; C_{arom}-OMe: 4.8 mmol/g; C_{arom}-O-C_{aliph} < 1 mmol/g; C_{arom}—O—C_{arom} ~ 1.9 mmol/g which means that the sum of β-O-4 linkages (C_{arom}—O—C_{aliph}) and 4-O-5 linkages (C_{arom}—O—C_{arom}) is circa 1.9 mmol/g in the initial lignin, both being almost in the same quantities around 0.9 mmol/g (1.9 divided by a factor of 2 for 4-O-5 ether linkage because 2 aromatic carbons are involved in one linkage).

Carboxylic groups (COOH) quantified by ^{1}H and ^{31}P NMR are respectively 0.6 and 0.8 mmol/g while the occurrence of COOR (including COOH) groups is 1.8 mmol/g by ^{13}C NMR, suggesting that ester groups COOR (with R ≠ H) represent around 1 mmol/g in the initial

lignin. Aromatic units are quantified at 5.7 mmol/g in the initial lignin; aromatic unit with a free OH group (phenolics) are 3.8 mmol/g thus around 1.9 mmol/g of remaining units do not possess free phenolic OH and this value is in total accordance with the previously obtained value of 1.9 mmol/g for possible ether linkages. From these data, we can draw an average representation of the aromatic units (^{13}C) in initial lignin, it might be an aromatic ring bearing two C_{arom}—C bonds, two C_{arom}—O bonds and two C_{arom}-H. If we consider 1 phenolic unit for 2.6 guaiacyl units and around 3–4 syringyl units (given by ^{31}P NMR) we can assume that condensed aromatic units with C_{arom}—C_{arom} linkages exist to explain the high ratio of C_{arom}—C bonds founded. Finally, the value of 5.7 mmol per g of aromatic units in the initial lignin might lead to 44 wt% of the initial material if we consider a "C_6H_6" unit, which means that starting from 30 g of lignin (including ashes) around 13 g of "C_6H_6" aromatic rings could be theoretically obtained if all the inter-units linkages were cleaved.

3.2. Hydroconversion reactions

The hydroconversion of the soda lignin over CoMoS/Al$_2$O$_3$ catalyst was performed at various residence times between 0 h (t_0) and 13 h, t_0 being the time where operating conditions (T = 350 °C and P = 8 MPa) were reached. First, this new semi-batch set-up has been demonstrated to be very powerful compared to the traditional batch system previously used [15], as we obtained, with the same CoMoS catalyst, the same conversion after only 5 h hours compared to 10 h with a conventional batch system. This result indicates a higher mass transfer of hydrogen from gas phase to liquid phase, thanks to the continuous feeding of H$_2$ that increases the driving force contribution in the mass transfer flow. Effectively, the continuous feeding of H$_2$ allowed to keep a stable partial pressure of H$_2$ during whole experiment which was not the case previously due to the increase of the light products in the reactor by increasing residence time. By the way, the available hydrogen in liquid phase permits the hydrogenolysis/hydrogenation reactions at the solid surface of the catalyst. Thanks to the condensing system, the rapid and continuous removing of water and light products from the reacting mixture was clearly observed and avoid long contact of catalyst with water and over-conversion of lighter liquid products to gas. The calculation of the conversion is always an issue for lignin valorisation studies because it depends greatly of the calculation method. In previous work, the lignin conversion was calculated considering that lignin residues were similar to starting lignin. However, compared to lignin, lignin residue is often highly modified and this value does not reflect the real effect. Using this method we obtained a conversion of 40 wt% at t0 while it reached 91 wt% after 13 h. If we use the conversion of lignin only based on remaining solid (THF-insolubles) versus ash- and moisture-free lignin, it is varying from 92% at the beginning of the run (t0) to 97% after 13 h. The catalytic hydroconversion experiments led to four different fractions in the batch reactor: gas, liquid, lignin residue, solids and two phases in the first separator/condenser: aqueous and organic phase (Fig. 1). The overall evolution of gases, liquids and solids (THF-solubles and THF-insolubles) in function of the residence time is given in Fig. 2. The total organic compounds represent the organic liquids both recovered from the reactor and the separator (tetralin and its derivatives have been deduced). Aqueous fraction is composed of water and a few water-soluble organic compounds. Organic liquid was the main product and its formation increased linearly from t_0 to 13 h, while THF-solubles (lignin residue) and THF insoluble (solids) decreased until reaching low values of 5.6 wt% and 3 wt% respectively. The gases and aqueous phase followed the same trend, a strong increase at the beginning and then after 2 h, a slower growing slope. H$_2$ consumption (mmol.g$_{lignin}^{-1}$) was measured and increased continuously with a strong slope from t_0 to 5 h and then slightly after 5 h (Fig. 3). The overall consumption during the 13 h of reaction is 43 mmol of H$_2$ per gram of lignin, thus 1.3 mol (2.6 g) of H$_2$; this H$_2$ incorporation in the products will increase the overall mass balance.
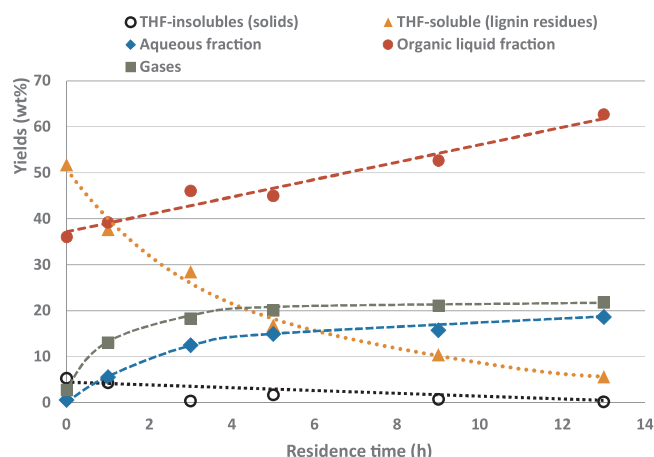
Fig. 2. Evolution of gases, liquids and solids yields (in wt% based on ash- and moisture-free initial lignin) during hydroconversion of lignin over CoMoS/Al_2O_3 in function of residence time.
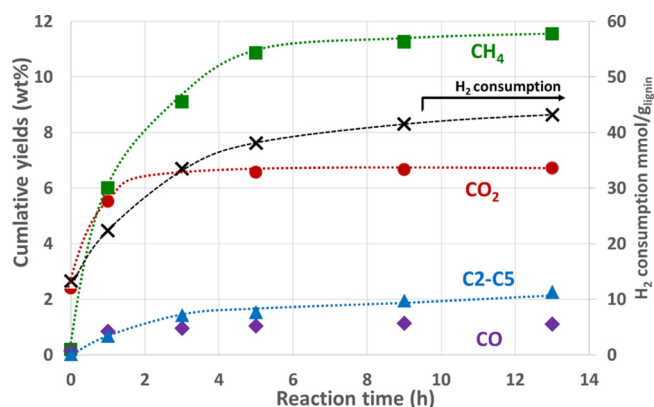

Fig. 3. Evolution of gases formed and H_2 consumed in wt% during the lignin hydroconversion on CoMoS/Al_2O_3 in function of residence time.

3.3. Gas products

The dynamic evolution of the different gaseous products in function of the residence time was measured online and the cumulative values are reported in Fig. 3. The main gases are CO_2 and CH_4 coming respectively from decarboxylation of carboxylic functions and from hydrogenation of CO_2 (methanation) or demethylation/demethoxylation of methoxy groups from syringyl and guaiacyl units. In addition, a few CO and C_2-C_6 hydrocarbons were detected. We observed that the CO_2 and CO were mainly early formed during the temperature increase of the first thermal stage and disappeared after 3 h of residence time suggesting the total conversion of carboxylic functions from the initial lignin. At the same time, following H_2 evolution, we clearly observed that the main part of H_2 consumption occurred (Fig. 3). The total amount of CO_2 formed represents 6.7 wt% of the initial lignin while the available COOH (^{31}P NMR) in the initial lignin would lead to a maximum of 3.5 wt% of CO_2 (1.05 g). However, we previously observed the presence of ester (-COOR) groups in the lignin that can be transformed by cleavage to carboxylic acids in those operating conditions, and then offer an additional possibility to form CO_2; the total (COOR + COOH) functions will lead to 8 wt% of CO_2. As aldehyde, carbonyl functions are approximately quantified at around 1.7 mmol/g in the initial lignin by ^{1}H NMR, this could explain the 1.1 wt% of CO most probably coming from the decarbonylation (DCO) of aldehydes or esters in competition with their hydrogenation [30], but it could also be formed by reverse water-gas-shift reaction and complete the balance for the initial carboxylic groups. The evolution of CH_4 obeyed to a similar trend but was

delayed compared to CO_2: methane was detected when reaction temperature was reached and disappeared after 6 h, the total amount formed being close to 11.5 wt% of the initial lignin. Regarding this behavior, it seems that CH_4 was not mainly coming from CO_2 hydrogenation (methanation) because it continues to be produced after 3 h. CH_4 was probably formed directly by demethylation reaction or demethoxylation process followed by hydrogenation of MeOH as it is commonly observed in guaiacol HDO reactions [31]. Effectively, due to the flowing configuration of the reactor, the gases being recovered as soon as they are formed and without extended contact with the catalyst, the hydrogenation of CO_2 to CO and CH_4 might be few. From detected methoxy groups (4.8 mmol/g), 2.3 g of methane can be formed which correspond to 8 wt% of initial lignin; thus the main part of methane is definitely coming from demethylation/demethoxylation reaction.

3.4. Solid products

Concerning the solids, the amount of THF-insoluble found after the heating period (at t0, 8.4 wt%) is not far from that of the initial THF-insoluble content measured in the initial lignin (9 wt% including ashes), but the elemental content of this solid is very different, O/C and H/C being already much lower after t0 (Fig. 4). This Figure provides Van Krevelen representation of the starting lignin (as well as its separation into two fractions) and the various soluble and insoluble lignin residues. It is observed that the first lignin residue (t_0) is totally different from the THF-soluble part of the lignin. We can observe that the insoluble part of lignin was also deeply transformed during heating period by losing O and H, which indicates clearly dehydration reactions. The same phenomenon was already observed with the same lignin by simple thermal conversion [32]. Afterwards, the solid part was converted continuously and the final ash-free solid residue after 13 h was 3.3 wt% of the initial ash-free lignin. Due to the low quantity and the insolubility of these solids in classical solvents including THF, only elemental characterization was performed on the insoluble fraction still containing ashes (Table 2). At t_0 point, the O content decreased to 23 wt% and the H content decreased from 3.6 wt% to 2.5 wt% while the C content remained around 40 wt%. During the 13 h of reaction, the C content decreased from 40 wt% to 16 wt% and H content decreased from 2.5 wt% to 1.3 wt% respectively while the O content decreased slightly from 23 wt% to 19 wt%. The high ratio of O/C suggests the formation of condensed phenolic moieties. Unsurprisingly, the ash content, evaluated by subtraction of the organic part, increased in function of reaction time. After 13 h, the organic fraction represented about 47.3 wt% of THF-insoluble solids, which means that the ash content reached 52.7 wt%, corresponding well to the initial ash content (3 wt% of initial feed).
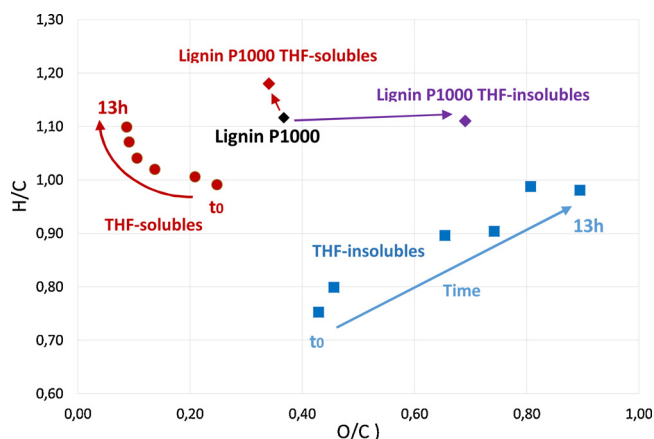

Fig. 4. Van Krevelen diagram (atomic O/C versus H/C) for lignin, lignin residues (THF-solubles) and solids (THF-insolubles).

Table 2

Elemental analyses, ashes content and O/C, H/C atomic ratios of the THF-insoluble fraction including ashes in function of residence time.

Residence time (Yield wt% ± 2 wt%)	0 h (11.3)	1 h (10.1)	3 h (6.3)	5 h (7.6)	9 h (6.7)	13 h (6.2)
C	40.5	34.9	22.5	27.1	19.0	16.2
H	2.5	2.3	1.7	2.0	1.6	1.3
O	23.2	21.2	22.3	23.6	20.4	19.3
N	1.0	0.8	0.5	0.6	0.4	0.3
S	6.1	6.5	9.1	8.1	9.4	10.2
Ashes (*)	26.7	34.3	43.8	38.5	49.2	52.7
Atomic ratios						
H/C	0.75	0.80	0.90	0.90	0.99	0.98
O/C	0.43	0.46	0.74	0.65	0.81	0.89

* Ashes deduced from CHONS.

3.5. Lignin residues

The lignin depolymerization can be easily followed by the evolution of the molecular masses given in PS equivalent by GPC analysis of the various lignin residues. We performed first the GPC analysis of the initial lignin after acetylation reaction [24] in order to dissolve it in THF solvent, and the GPC analysis of the soluble part of the initial lignin in THF (Fig. 5). We can see a great difference between those two distributions due to the insoluble part of the initial lignin and to the slight weight increase expected with the acetylation step. Compared to the acetylated lignin, there is a strong decrease of the average molecular mass after reaching the reaction temperature (t_0) but the GPC of this lignin residue is very close of that of the THF-soluble part of the initial lignin. A slight continuous decrease was observed by increasing the residence time. According to the obtained curves, the Mw (weight average) decreased from 3067 g.mol^{-1} PS equivalent to 1090 g.mol^{-1} PS eq. after 13 h while the Mn (number average) varied from 970 to 540 g.mol^{-1} PS equivalent and polydispersity decreased from 3.2 to 2. However, the decrease of molecular weights reached a plateau after 5 h and does not vary much between 5 h and 13 h. The polydispersity remains around 2 during the whole reaction. Atomic O/C and H/C ratios decreased strongly at the very beginning of the reaction consistent with decarboxylation (two oxygens for one carbon loss) and dehydration (1 oxygen and 2 hydrogens, no carbon loss). As the molar masses were shortened, as seen by GPC, we can assume that not only O and H were removed through CO_2 and H_2O but also C—O and C—C cleavages occurred releasing some monomers or oligomers.
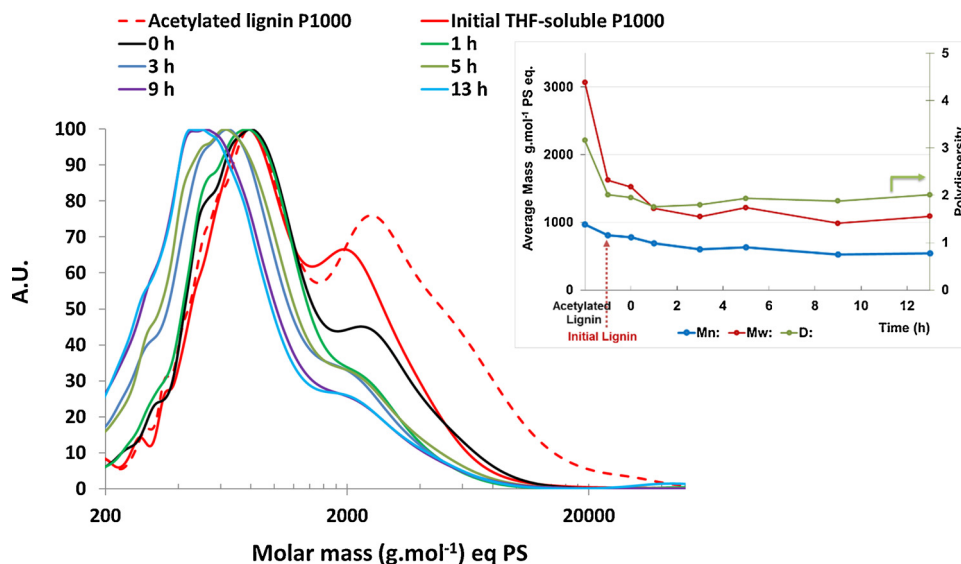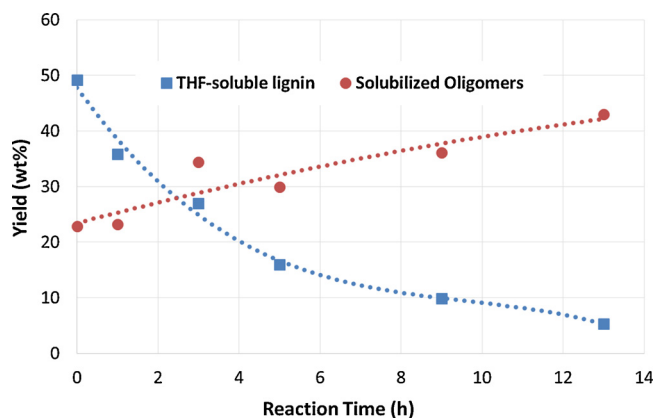

Fig. 6. Distribution of lignin residues solubilized in liquids (oligomers) and THF-solubles.

A part of this lignin residue is soluble in the liquid mixture and was not separated from the organic fraction during the centrifugation step. Thanks to a previously developed protocol including heptane precipitation, this fraction was recovered from the liquid and the evolution of this miscible part in liquid is given in Fig. 6. We observed that this liquid-miscible fraction, composed by lignin oligomers, increased in the liquid phase while THF-soluble fraction decreased and reach a low value (5 wt%) after 13 h. Their molar masses distribution compared to residual lignin at 13 h indicates a similar profile in the region of 600 < Mw < 1300 g/mol PS eq. but a loss of higher masses (1300–10000 g/mol PS eq.) while the presence of lower masses (200–600 g/mol PS eq.) was detected probably due to the remaining part of liquid on these solids after centrifugation (Fig. 7). It can be noticed that elemental composition and organic functions detected by ^{31}P NMR present on miscible oligomers and THF-soluble lignin residues are very similar (Table 3 and Figure S1). We can thus conclude that these oligomeric fractions miscible in organic liquid possess the same chemical structure as lignin residues (THF-solubles) but are simply composed of shorter chains.

The evolution of ^{13}C NMR of the THF-soluble lignin residues (Fig. 8a) indicated that the C_{aliph}-O ($-OCH_3$ not included) including ether bonds as well as the aliphatic OH, and the −COOR functions (carboxylic acids and esters) were quickly cleaved or converted during the heating stage. The corresponding expected yield of CO_2 is 8 wt%. Experimentally, we only got 2.4 wt% for CO_2 at t_0 indicating that a part

Fig. 5. GPC analysis of lignin residues in function of residence time.
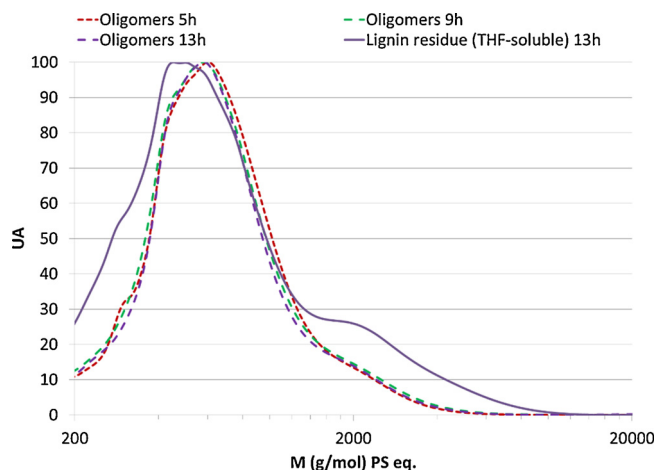
Fig. 7. GPC analyses of oligomers soluble in organic liquid fraction at 3 h, 5 h, 9 h, and 13 h compared to THF-soluble lignin residue after 13 h.

Table 3
Elemental analyses and O/C, H/C atomic ratios of the THF-soluble fraction and precipitated oligomers in function of residence time.

	THF-soluble lignin residues				Miscible oligomers (Precipitated lignin)			
Residence time (h)	3	5	9	13	3	5	9	13
C	78.6	80.9	82.5	81.8	77.8	80.5	82.1	83.6
H	6.7	7.0	7.4	7.5	6.9	7.2	7.0	7.3
O	14.4	11.4	10.1	9.5	14.3	11.8	11.1	9.2
N	1.1	1.3	1.3	1.3	1.0	1.2	1.3	1.4
S	0.1	0.1	0.1	0.1	0.2	0.1	0.11	0.0
Total	100.9	100.8	101.3	100.2	100.2	100.8	101.6	101.6
Atomic ratio								
H/C	1.02	1.04	1.07	1.10	1.07	1.07	1.02	1.05
O/C	0.14	0.11	0.09	0.09	0.14	0.11	0.10	0.08

of $-COOR$ groups were not converted by decarboxylation but released into the liquid phase or/and hydrogenated. By GC × GC analysis, some fatty ester and carboxylic acid compounds were effectively clearly detected in the liquid phase at short reaction time. The decrease of $-OCH_3$ in the THF-soluble was also observed during the heating period and until 3 h. This observation is in accordance with the high concentration of methoxy-substituted phenols in the liquid phase observed below and the rapid formation of CH_4 during the same period. The decrease of $C_{arom}-O$, $C_{arom}-H$ and $C_{arom}-C$ followed the same parallel trend, a strong decrease during the heating period, a moderate decrease from t_0 to 5 h and a slow decrease after 5 h until 13 h. During $\beta-O-4$ or 4-O-5 ether inter-unit cleavage, $C_{aromatic}-O-R$ was converted to $C_{aromatic}-O-H$ and possibly transferred to the liquid phase but the aromatic units still remain with the same number of $C_{aromatic}-O(H)$, $C_{aromatic}-H$ and $C_{aromatic}-C$ bonds which completely agreed with ^{13}C NMR observations. However, $C_{aromatic}-C$ decreased less than $C_{aromatic}-O$ and $C_{aromatic}-H$, suggesting that the aromatic units remaining in lignin residues are less oxygenated and more alkylated (methylation reaction) or condensed with $C_{arom}-C_{arom}$ bonds inter-units. Finally, aliphatic carbons which are present on alkyl chains between units but also as fatty chains decreased following a similar trend as aromatic units (Fig. 8a). ^{31}P NMR after phosphitylation of lignin residues (Fig. 8b) showed also clearly the strong disappearance of aliphatic OH and carboxylic acids during the temperature increase step leading to water and CO_2, while the other types of OH (phenolic) are slowly decreasing during the 13 h. All the methoxy-phenolics and condensed-phenol units were converted during the experiments leading to simple phenolics which are remaining at the same level until 5 h and then start to decrease.
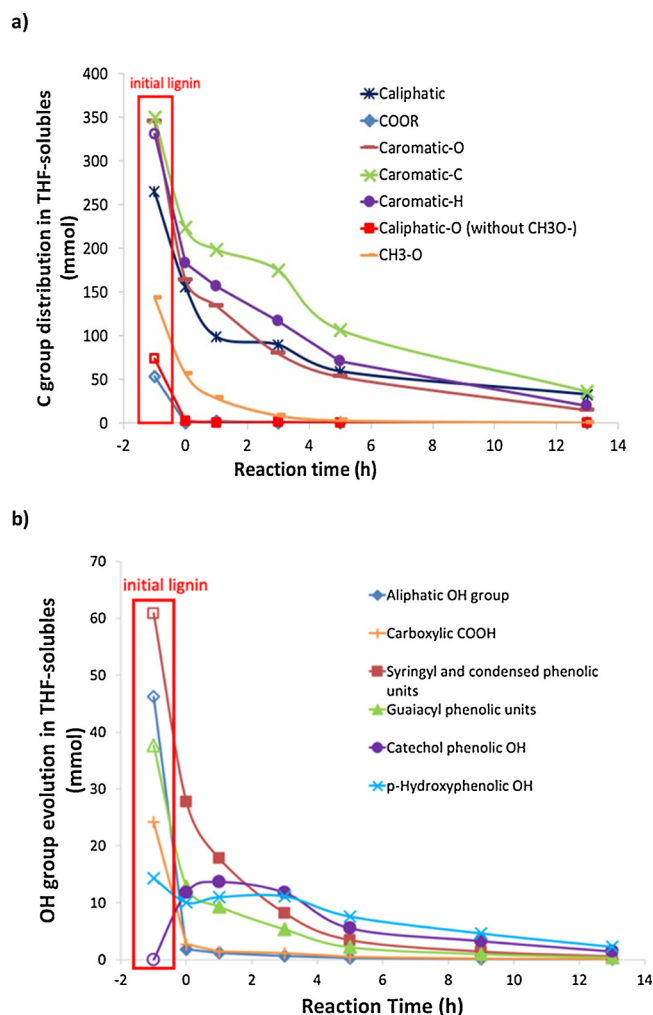

Fig. 8. ^{13}C and ^{31}P (after phosphytilation) NMR analysis of lignin residues (THF-soluble) showing evolution of C and $-OH$ functions in mmol compared to the initial lignin.

These results are consistent with the expected rates of each reaction: dehydration and decarboxylation are the faster reactions in those operating conditions and occurred during the heating step of the reactor as well as ether cleavage (β-O-4, 4-O-5) releasing phenolics in the liquid, demethoxylation and demethylation, both possible in those conditions, are rapid but slowest and occurred subsequently. However, as phenolic units are continuously released into the liquid phase, it is suggested that some more resistant C—C inter-unit bonds cleavage still occurred lately but these linkages are not well identified. Similarly, ^1H NMR evolution showed that only aromatic and aliphatic protons are remaining in lignin residue with few phenolic groups (Figure S2, suppl. mater.).

Finally, after 13 h the lignin residue resulting from both inter-unit bond cleavage and chemical transformation is a smaller lignin fragment partially deoxygenated, without $C_{aliphatic}$-O (ether or alcohol) and carboxylic functions but still having aromatic units with a few remaining OH groups (phenol) and aliphatic carbons chains.

3.6. Liquid fraction

Regarding the total liquid phase, including both organic and aqueous fractions, the total yield reached 81.6 wt% (based on moisture-free and ash-free lignin) after 13 h (Fig. 2). In the starting lignin (around 29 g), 46.2 mmol of aliphatic OH have been detected by ^{31}P NMR (Fig. 8b), this value would lead to 0.83 g of water after total
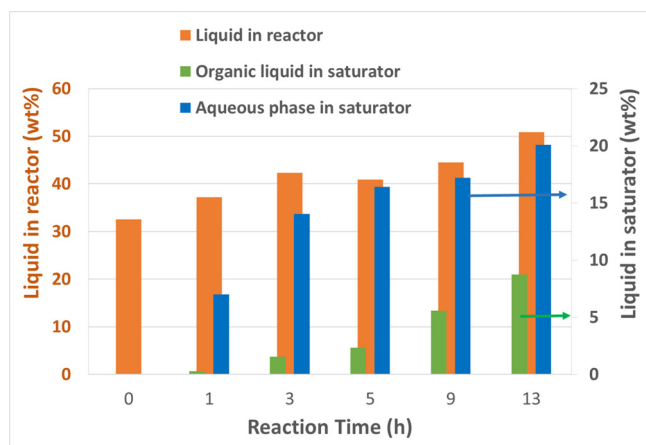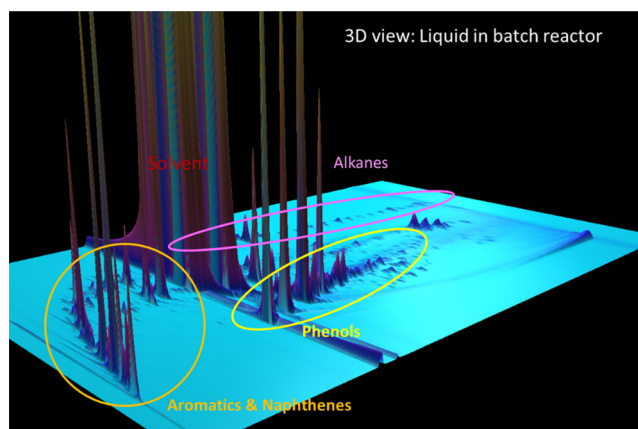
Fig. 9. Evolution of organic liquid phase in the reactor and organic and aqueous phases in the separator.

a)

b)

Fig. 10. Fig. 10. 3D-view of the GCxGC chromatograms of organic liquid phase after 5 h in reactor (a) and in separator (b).
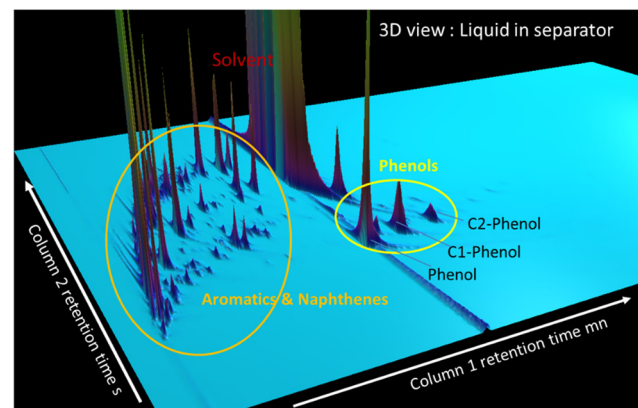
dehydration. If we add all the OH groups from phenolic units (H, S, G) the value would increase up to 2.86 g. More phenolic units are expected to be formed during the catalytic process by the cleavage of aromatic ethers also present in the initial lignin. Thanks to the reflux system, the quantity of aqueous phase transferred in the separator was evaluated after decantation and separation with organic phase (Fig. 9); this aqueous fraction is mainly composed of water (95 wt%) and around 4 wt% of carbon, according to Karl Fischer and elemental CHONS analyses (Table S8, suppl. mater.). GCxGC analysis of the aqueous phase revealed the presence of water-soluble organic compounds like ketones, aldehydes, alcohols and small carboxylic acids (not shown). However, the water formed in the reactor during the heating period and before 1 h is not easily quantified. Using Karl-Fischer titration of organic liquid, a water content of 1.4 wt% was measured at t_0 in the reactor corresponding to 1.1 g (Table S9, suppl. mater.). We can also observe the continuous increase of organic and aqueous phase in the reactor until 13 h.

For most of the studies on lignin conversion, the liquid phase is always the most challenging part to analyze because of the complexity of the mixture. In our work, the monomers produced from lignin are quite numerous and diverse and the liquid contained also a significant amount of tetralin solvent and its derivatives and the miscible oligomers previously mentioned. The shape of the organic liquid curve suggest that monomers and oligomers are linearly formed until 13 h and do not reach a plateau which means that depolymerization still occurs at that time. The detailed monomers composition in the liquid was investigated by GCxGC using chemical family group methodology. Of course, as 1D-GC, this comprehensive technique does not allow to identify components which are not vaporizable, in general components until 22–32 carbons can be detected depending of organic functions. The main monomers families identified thanks to the mass detector (GCxGC-MS) were dimethoxyphenols, methoxyphenols, phenols, alkanes, naphthenes and aromatics (BTX) [15]. From the 3D-view of GCxGC analyses (Fig. 10), we observed very clearly that the lighter products (BTX, naphthenes and small phenols) were mainly obtained in the separator while, in the reactor, remained mostly heavier compounds including long-chain alkanes, alkylphenolics and tetralin derivatives. The presence of long chain alkanes is undoubtedly due to the occurrence of cutin and suberin moieties cross-linked to lignin fragment [33] and containing fatty esters or carboxylic acids that are readily transformed into long chain alkanes in those operating conditions.

The general evolution of the monomers in the total liquid phase is given in Fig. 1a; each curve of this figure was obtained by the sum of the corresponding monomers in the reactor (Figs. 11c) and in the separator (Fig. 11b). Dimethoxy- and methoxyphenols are only quantified in the reactor organic fraction. As previously observed in lignin residues, these monomers are rapidly converted in the reactor during the first 5 h of reaction and then they are not detected anymore in organic liquid. This result indicates clearly that the methoxyphenolic monomers coming from the cleavage of lignin units were efficiently converted to alkyphenols, which are also formed by the cleavage of H-unit of the lignin. As benzenediols (catechols) were detected in very low quantities, it seems that (di)methoxyphenols were mainly converted by demethoxylation to alkylphenols. From early studies on guaiacol as model molecule for HDO, we effectively observed that contrarily to demethylation that can occur without catalyst at 350 °C, demethoxylation requires the presence of a catalyst [31]. Alkylphenols were the main monomers products in the liquid phase and increased to reach a plateau at around 10 h. In the reactor, we can observe a decrease around 5 h while the alkylphenols appeared and increased in the separator (Figure S3, suppl. mater.). However, the alkylphenols family recovered in the separator was mainly composed of phenol, C_1- and C_2-phenol, C_3- and C_4-phenols being detected as traces (Figure S4, suppl. mater.). The main part of aromatics and naphthenic compounds was recovered in the separator contrarily to phenols which mainly remain in the reactor mixture (Figure S3, Suppl. mater.). We also observed that naphthenes and aromatics started to be transferred in the separator after 1 h while it takes 3 h for phenol because of the higher boiling point. These figures show clearly the efficiency of the separating system which allow to recover most of the deoxygenated products and a few part of lighter phenols in the separator while heavier phenols and other monomers stayed in the reactor tank with dimers and oligomers. Concerning the alkyl-substitution state of the formed monomers, it can be noted that C_2-derivatives are always the most abundant in the various
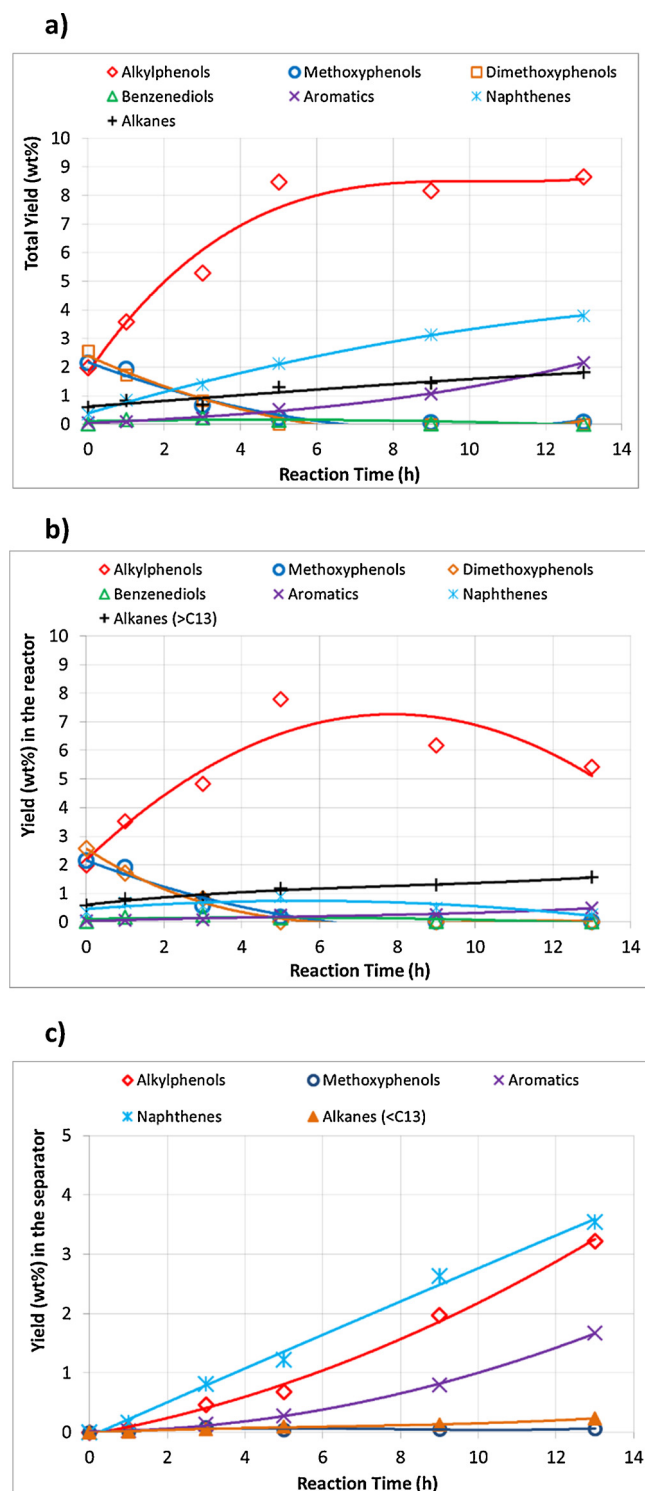
a)

b)

c)

Fig. 11. Evolution of monomers products in organic liquid phase (a) total; (b) in the reactor; (c) in the separator in function of residence time.

families as illustrated for phenol, aromatics and naphthenes (Figure S5, suppl. mater.) whereas the logical derivative would be the C_3-derivatives if the main units in the lignin were phenyl propane as generally proposed for lignin structure. However, this lignin is not a native lignin and two hypotheses can be made: the units are mainly connected via propyl chain but the γ-carbon (CH_2-OH) can be easily removed in those operating conditions; or, the ferulic and coumaric units were highly present in the lignin structure and gave ethyl-derivatives (Scheme S1, suppl. mat.) which is in accordance with the source of the

lignin used [34]. Effectively, the lignin coming from wheat straw is not only composed of the three syringyl, guaiacyl and phenolic units but also contains ferulic and *p*-coumaric acids cross-linked with lignin fragment, as well as cutin and suberin moieties which are made of C_{16}-C_{18} fatty esters [35,36]. Those esters are progressively converted to carboxylic acids and alkanes in the liquid phase. In early works on model molecules conversion, it was reported that carboxylic acids or esters were converted to alkanes and alkenes on sulfide catalyst under H_2 pressure by two pathways hydrodeoxygenation/hydrogenation (HDO) and decarbonylation/decarboxylation (DCO) [30,37]. The first hydrogenation route lead to alkanes or alkenes with the same number of carbons via the corresponding alcohol; the second pathway is the decarbonylation/decarboxylation route leading to alkenes/alkanes with one carbon less by loss of CO or CO_2. The main route observed with NiMoS and CoMoS catalysts was HDO and few CO_2 was observed, CO being the main gas formed. We observed here that alkanes C_{13+} present in the liquid are mainly C_{15} to C_{18} and then C_{28} to C_{32} (the C_{32} alkane is the last detected alkane in our GCxGC conditions) were also detected (Figure S7, sup. mater.). If the initial size of these esters in lignin are C_{16}-C_{18} as reported, the presence of alkanes with 15 and 17 carbons confirm the decarboxylation route while C_{16} and C_{18} alkanes would be issued from hydrogenation pathway. The longer C_{28-32} alkanes are formed by ketonization reaction between two molecules of C_{16}-C_{18} carboxylic acids with loss of one molecule of CO_2. However, the decrease of OH from carboxylic acid functions in lignin is around 24 mmol while the loss of CO_2 corresponding to alkanes C13+ formation (based on alkanes quantification) would correspond to a maximum of 1.4 mmol. Thus it is evidenced that the high quantity of CO_2 formed is mainly coming from ferulic/coumaric units and not from fatty esters.

Finally, 4.9 g total monomers were quantified after 13 h of catalytic hydroconversion which represents 17 wt% of initial lignin. Among those monomers, 4.4 g (15.4 wt%) are coming from aromatic units in the starting lignin; this value has to be compared with the 44 wt% of "C_6H_6" aromatic units theoretically available in the starting material. The 30 wt% aromatic units remaining are undoubtedly in the oligomeric fraction which can be divided in two phases: the precipitated miscible oligomers described previously and the non-detected compounds. This late fraction can be composed by oligomers that are shorter and thus not isolated by heptane addition and also by the volatile organic compounds possibly formed during the catalytic process, like methanol, and probably lost during the products-recovery protocol. The ether inter-units linkages detected in the initial lignin were broken leading to monomers and oligomers but then, the formed oligomers are composed of aromatic units linked by stronger C—C bonds more difficult to cleave and the evolution to monomers and shorter oligomers is reduced but still observed. Finally, based on these results, we can propose a general reaction scheme to illustrate the different steps already described during the catalytic hydroconversion of the lignin in our operating conditions (Fig. 12). It can be noticed that the same chemical transformation were observed on lignin residues and monomers which signify that the catalyst interact with both materials.

3.7. Catalyst after lignin hydroconversion

Thanks to their extrudated shape, the catalysts were recovered from the solids after Soxhlet THF washing, and, CHONS elemental analyses, XPS and textural analyses were performed. The C content in the used catalysts increased to around 12% from 1 h to 13 h of reaction showing that the catalyst was rapidly coked at the very beginning of the process and then remains at the same level of C during all the process (Table S5 suppl. mater). We can assume that the deposit of carbon is coke because the catalysts were intensively washed with THF and the carbon physisorbed species would have been removed during this step. On the same way, S content decreased to 6% during the heating step and then stayed stable during the 13 h. The same phenomenon was observed for textural
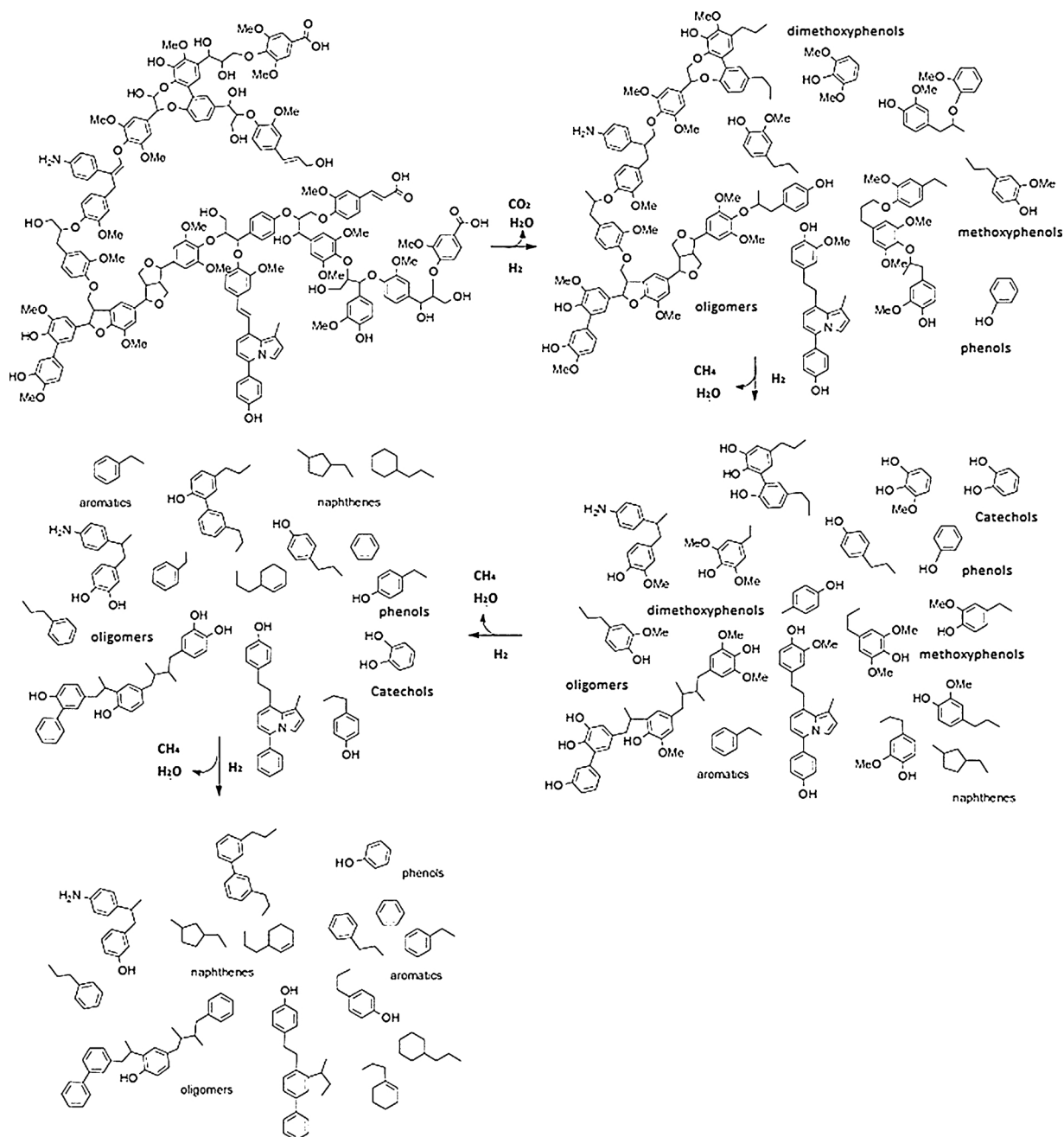
Fig. 12. Illustration of the general reaction scheme during lignin catalytic hydroconversion over CoMoS/Al$_2$O$_3$ (fatty esters coming from suberin/cutin entities have been omitted for clarity).

properties (Table S5, Figure S6 suppl. mater.). During the heating period, the total pores volume and BET surface area decreased to reach lower values which are kept during all the process. The BET surface decreased to 180 m^2.g^{-1} which is not so far from the initial catalyst while the pore volume decreased from 0.47 to 0.29 and the average pore size is around 6 nm compared to 7.9 in the initial catalyst.

The XPS elemental analyses (Table S6, suppl. mater.) of the catalysts after reaction showed also a decrease of the S content at the surface of the catalyst after reaching the reaction temperature but, then, a stable level of S at the surface of the catalyst between 0 h and 3 h. In addition, according the XPS decomposition (Table S7, suppl. mater.) the same amount of Mo$^{(IV)}$ (MoS$_2$) was detected for the used catalysts after 0 h, 1 h and 3 h. Of course, this proportion of MoS$_2$ (63%) is lower than the freshly sulfided initial catalyst (83%) but the used catalysts were not re-sulfided after test but simply washed and kept under air; regarding the

S$_{2P}$ analysis, sulfate were found, confirming partial oxidation at the surface. Thus, we can note that the main changes on the catalyst occurred during the heating period where lignin starts to be cleaved and transformed releasing mainly CO$_2$, water, methoxyphenolic monomers and oligomers. With our set-up system, gases are only briefly in contact with the catalyst as they are rapidly and continuously removed from the reacting mixture. The formation of water in the reactor during the heating period has been evaluated by Karl-Fischer titration and the reflux system does not allow to remove formed water until reaction temperature was reached; this amount of water (evaluated at around 1 g) could be in close contact with the catalyst before being transferred to the separator when the temperature of 350 °C was reached. We also know that THF-soluble lignin residue is one of the main product during this period, and, as seen by ^{31}P NMR of this fraction, aliphatic OH were strongly impacted during this step which indicate that quite high

quantity of water was formed in the liquid. Thus, the catalyst during the heating period could interact with water and phenolic oligomers/monomers. Nevertheless the used catalyst remained sulfided, with still a good S/Mo ratio for CoMoS phase. It still has a large surface area and an acceptable porosity. The pores are not entirely blocked by the carbon deposit and active site (MoS_2) are still available. The catalyst is impacted but still have a strong effect on the selectivity of the process as phenolics compounds are gradually converted by hydrodeoxygenation to aromatic and naphthenic compounds as expected even if the process is slow.

The catalyst used here is not the most efficient catalyst for obtaining aromatics and of course, performances can be certainly improved. However this catalyst is very resistant in our operating conditions and was not deeply modified after catalytic test. The effect of the presence of few H_2S in the gas phase to keep the sulfiding state of the catalyst was not evaluated yet but will be the object of further studies. From this experimental study on catalytic hydroconversion of a soda lignin, and thanks to the methodology and developed analytic tools, a kinetic network of the lignin depolymerization by catalytic hydroconversion is proposed and a lumped kinetic model was built for this reaction [23].

4. Conclusions

The semi-continuous reactor and a complete analysis methodology developed in this work allowed a better description of the reactivity of lignin which was efficiently converted to liquid monomers and oligomers with the help of a CoMoS/Al_2O_3 catalyst. During the heating period, decarboxylation, decarbonylation and dehydration reactions occurred rapidly followed by demethylation and lead to the early production of CO_2, CO, water and CH. In this early stage and until 13 h, the depolymerization of lignin was observed releasing continuously monomers and oligomers in the liquid fraction. Those rapid and mainly thermal processes were followed by demethoxylation and deoxygenation of methoxyphenols which are slower catalyzed-transformations in our operating conditions (T = 350 °C, P = 8 MPa). The light deoxygenated components as aromatics and naphthenes are very efficiently removed from the mixture also with produced water, which constitutes a good way to separate the targeted products, avoid over-conversion of the products and protect the catalyst from the presence of water. Finally, the production of phenols and BTX is less than expected but those experimental data allowed to better understand the chemical processes occurring during the hydroconversion reaction and could help to develop new catalysts. A complete reaction scheme for the catalytic hydroconversion of lignin was proposed and all these experimental results and kinetic data was further used to implement a lumped kinetic model.

Appendix A. Supplementary data

Supplementary material related to this article can be found, in the online version, at doi:https://doi.org/10.1016/j.apcatb.2019.117769.

References

[1] A.J. Ragauskas, G.T. Beckham, M.J. Biddy, R. Chandra, F. Chen, M.F. Davis, B.H. Davison, R.A. Dixon, P. Gilna, M. Keller, P. Langan, A.K. Naskar, J.N. Sadler, T.J. Tschaplinski, G.A. Tuskan, C.E. Wyman, Lignin Valorization improving lignin

[2] H. Wang, Y. Pu, A. Ragauskas, B. Yang, From lignin to valuable products-strategies, challenges, and prospects, Bioresour. Technol. Rep. (2018), https://doi.org/10.1016/j.biortech.2018.09.072.

[3] K.V. Sarkanen, H.L. Hergert, Lignins, occurrence, formation, in: K.V. Sarkanen, C.H. Ludwig (Eds.), Structure and Reactions, Wiley Interscience, 1971, p. 43.

[4] J. Zakzeski, P.C.A. Bruijnincx, A.L. Jongerius, B.M. Weckhuysen, The catalytic valorization of lignin for the production of renewable chemicals, Chem. Rev. 110 (2010) 3552–3599, https://doi.org/10.1021/cr900354u.

[5] F.G. Calvo-Flores, J.A. Dobado, J. Isac-García, F.J. Martín-Martínez, Isolation of Lignins, in Lignin and Lignans As Renewable Raw Materials, (2015), pp. 113–144.

[6] M.P. Pandey, C.S. Kim, Lignin depolymerization and conversion: a review of thermochemical methods, Chem. Eng. Technol. 34 (2011) 29–41, https://doi.org/10.1002/ceat.201000270.

[7] B. Joffres, D. Laurenti, N. Charon, A. Daudin, A. Quignard, C. Geantet, Thermochemical conversion of lignin for fuels and chemicals: a review, Oil Gas Sci. Technol. 68 (4) (2013) 753–763, https://doi.org/10.2516/ogst/2013132.

[8] T. Vangeel, W. Schutyser, T. Renders, B.F. Sels, Perspective on lignin oxidation: advances, challenges and future directions, Top. Curr. Chem. J. 376 (4) (2018) 30, https://doi.org/10.1007/s41061-018-0207-2.

[9] D. Meier, R. Ante, O. Faix, Catalytic hydropyrolysis of lignin: influence of reaction conditions on the formation and composition of liquid products, Bioresour. Technol. Rep. 40 (1992) 171–177, https://doi.org/10.1016/j.biortech.2018.07.028.

[10] N. Vasilakos, D.M. Ausigen, Hydrogen-donor solvents in biomass liquefaction, Ind. Eng. Chem. Process Dev. 24 (1995) 304–311.

[11] M. Kleinert, J.R. Gasso, T. Barth, Optimizing solvolysis conditions for integrated depolymerisation and hydrodeoxygenation of lignin to produce liquid biofuel, J. Anal. Appl. Pyrolysis 85 (2009) 108–117.

[12] F. Davouszadeh, B. Smith, E. Avni, R.W. Coughlin, Depolymerization of lignin at low pressure using lewis acid catalysts and under high pressure using hydrogen donor solvents, Holzforschung 39 (1985) 159–166.

[13] D. Meier, J. Berns, C. Gründwald, O. Faix, Analytical pyrolysis and semi-continuous catalytic hydropyrolysis of organocell lignin, J. Anal. Appl. Pyrolysis 25 (1993) 335–347.

[14] R.W. Thring, J. Breau, Hydrocracking of solvolysis lignin in a batch reactor, Fuel 75 (7) (1996) 795–800, https://doi.org/10.1016/0016-2361(96)00036-1.

[15] B. Joffres, C. Lorentz, M. Vidalie, D. Laurenti, A.A. Quoineaud, N. Charon, A. Daudin, A. Quignard, C. Geantet, Appl. Catal. B: Environ. 145 (2014) 167–176, https://doi.org/10.1016/j.apcatb.2013.01.039.

[16] B. Joffres, M.T. Nguyen, D. Laurenti, C. Lorentz, V. Souchon, N. Charon, A. Daudin, A. Quignard, C. Geantet, Appl. Catal. B: Environ. 184 (2016) 153–162, https://doi.org/10.1016/j.apcatb.2015.11.005.

[17] M.R. Haverly, K.V. Okoren, R.C. Brown, Optimization of phenolic monomer production from solvent liquefaction of lignin, ACS Sustain. Chem. Eng. 6 (2018) 12675–12683.

[18] M.J. Biddy, C. Scarlata, C. Kinchin, Chemicals from biomass: a market assessment of bioproducts with near-term potential, NREL Tech. Rep. (2016).

[19] C.R. Kumar, N. Anand, A. Kloekhorst, C. Cannilla, G. Bonura, F. Frusteri, K. Barta, H.J. Heeres, Solvent free depolymerization of Kraft lignin to alkyl-phenolics using supported NiMo and CoMo catalysts, Green Chem. 17 (2015) 4851–5092.

[20] A. Kloekhorst, J. Wildschut, H.J. Heeres, Catalytic hydrotreatment of pyrolytic lignins to give alkylphenolics and aromatics using a supported Ru catalystCatal, Sci. Technol. 4 (2014) 2367–2377.

[21] X. Huang, T.I. Koranyi, M.D. Boot, E.M.J.M. Hensen, Catalytic depolymerization of lignin in supercritical ethanol, ChemSusChem 7 (2014) 2276–2288.

[22] R. Rinaldi, R. Jastrzebski, M.T. Clough, J. Ralph, M. Kennema, P.C.A. Bruijnincx, B.M. Weckhuysen, Paving the way for lignin valorisation: recent advances in bioengineering, biorefining and catalysis, Agew. Chem. Int. Ed. 55 (2016) 8164–8215.

[23] J. Pu, D. Laurenti, C. Geantet, M. Tayakout-Fayolle, I. Pitault, Kinetic modeling of lignin catalytic hydroconversion in a semi-batch reactor. Article submitted to Special Issue "GLS-14", Chem. Eng. J. (2019) under press.

[24] W.G. Glasser, V. Dave, Molecular weight distribution of (semi-) commercial lignin derivatives, J. Wood Chem. Technol. 13 (4) (1993) 545–559.

[25] D.S. Argyropoulos, Quantitative phosphorus-31 NMR analysis of lignin: a new tool for the lignin chemist, J. Wood Chem.Technol. 14 (1994) 45–63.

[26] A. Granata, D.S. Argyropoulos, 2-Chloro-4,4,5,5-tetramethyl-1,3,2-dioxaphospholate, a reagent for the accurate determination of the uncondensed and condensed phenolic moieties in lignins, J. Agric. Food Chem. 43 (1995) 1538–1544.

[27] G. Toussaint, C. Lorentz, M. Vrinat, C. Geantet, Comprehensive 2D chromatography with mass spectrometry: a powerful tool for following the hydrotreatment of a Straight Run Gas Oil, Anal. Methods 3 (2011) 2743–2748, https://doi.org/10.1039/C1AY05045A.

[28] B. Omais, M. Courtiade, N. Charon, D. Thiébaut, A. Quignard, M.-C. Hennion, Investigating comprehensive two-dimensional gas chromatography conditions to optimize the separation of oxygenated compounds in a direct coal liquefaction middle distillate, J. Chromatogr. A 1218 (2011) 3233–3240, https://doi.org/10.1016/j.chroma.2010.12.049.

[29] K. Schofield, The enigmatic mechanism of the flame ionization detector: its overlooked implications for fossil fuel combustion modeling, Prog. Energ. Combust. Sci. 34 (2008) 330–350.

[30] M. Ruinard de Brimont, C. Dupont, A. Daudin, C. Geantet, P. Raybaud, Deoxygenation mechanisms on Ni-promoted MoS2 bulk catalysts : a combined experimental and theoretical study, J. Catal. 286 (2012) 153–164.

[31] V.N. Bui, D. Laurenti, P. Afanasiev, C. Geantet, Hydrodeoxygenation of Guaiacol

with CoMo catalysts Part I: promoting effect of Cobalt on HDO selectivity and activity, Appl. Catal. B: Env. 101 (3-4) (2011) 239–245.

[32] B. Shrestha, Y. le Brech, T. Ghislain, S. Leclerc, V. Carré, F. Aubriet, S. Hoppe, P. Marchal, S. Pontvianne, N. Brosse, A. Dufour, A multitechnique characterization of lignin softening and pyrolysis, ACS Sustain. Chem. Eng. 5 (2017) 6940–6949, https://doi.org/10.1021/acssuschemeng.7b01130.

[33] F. Xu, Structure, Ultrastructure and Chemical Composition in Cereal Straw As a Resource for Sustainable Biomaterials and Biofuels, R.-C. Sun, Elsevier Ed, 2010.

[34] G.X. Pan, J.L. Bolton, G.J. Leary, Determination of Ferulic and p-Coumaric acids in Wheat Straw and the amounts released by mild and alkaline peroxide treatment, J. Agric. Food Chem. 46 (1998) 5283–5288.

[35] A. Scalbert, B. Monties, J.-Y. Lallemand, E. Guittet, C. Rolando, Ether linkage between phenolic acids and lignin fractions from wheat straw, Phytochem. 24 (1985) 1359–1362.

[36] C. Crestini, D.S. Argyropoulos, Structural analysis of wheat straw lignin by quantitative ^{31}P and 2D NMR spectroscopy. The occurrence of ester bonds and β-O-4 substructures, J. Agric. Food Chem. 45 (1997) 1212–1219, https://doi.org/10.1021/jf960568k.

[37] S. Brillouet, E. Baltag, S. Brunet, F. Richard, Deoxygenation of decanoic acid and its main intermediates over unpromoted and promoted sulfided catalysts, Appl. Catal. B: Environ. 148-149 (2014) 201–211.